



Loss Modeling for 2017 Sarpol-e Zahab Earthquake

Parisa Shahbazi¹ and Babak Mansouri^{2*}

1. Ph.D. Candidate, International Institute of Earthquake Engineering and Seismology (IIEES), Tehran, Iran

2. Associate Professor, Earthquake Risk Management Research Center, International Institute of Earthquake Engineering and Seismology (IIEES), Tehran, Iran,

* Corresponding Author; email: mansouri@iiees.ac.ir

Received: 29/07/2018

Accepted: 29/08/2018

ABSTRACT

The November 12, 2017 Sarpol-e Zahab earthquake (M_w 7.3) occurred at 18:18 GMT (21:48 local time) and affected vastly the western part of Iran especially the Kermanshah province. The death toll was at least 620, the total number of injured people just the day after the earthquake was 5346 and around 70000 people were left homeless. This study aims to estimate the distribution of physical damages to the building stock using our domestic model and to calculate and validate the associated casualties under Sarpol-e Zahab earthquake event using a global model with some modifications. This region has been chosen because it has suffered major losses due to the recorded high PGA value of 684 gal and also due to the fact that some adequate field surveys and documentations were completed for this event. Since accurate building distribution maps are not available or accessible, to develop a spatial building database, a dasymetric mapping technique has been employed by merging a grid world population distribution map and the national census data. OpenQuake platform is utilized to simulate the ground motion field and to assess the physical damages and human loss. The results were compared with the actual observed data and showed relatively a proper match.

Keywords:

Sarpol-e Zahab earthquake; Seismic hazard; Loss modeling; Physical damage; Human loss; OpenQuake

1. Introduction

A severe earthquake of M_w 7.3 struck western part of Iran especially Kermanshah province on 2017.11.12 at 21:48 local time, at a depth of approximately 18 km. Since the earthquake ruptured near Sarpol-e Zahab city (37 km), it is named as "Sarpol-e Zahab Earthquake". IRSC (Iranian Seismological Center) reported that the epicenter was located at 34.77°N and 45.76°E [1]. According to USGS (United States Geological Survey) analysis, the earthquake was an oblique-thrust-faulting event, the nodal plane of which had a strike, dip and rake angles of 351°, 16° and 137° respectively [2]. IIEES (International Institute of Earthquake Engineering and Seismology) report indicated that one section of

MFF (Mountain Front Fault) faults with a lower dip angle (10° to 15°) plane caused the event [3].

For this event, 112 accelerograms were recorded in Iran. The maximum recorded peak ground acceleration was 684 gal (almost 0.697 g) at SPZ station, which is the nearest station to the epicenter, located at 34.46°N and 45.87°E, Sarpol-e Zahab city, with V_{s30} equal to 619 m/s [4]. The intensity of ground motion in that area is found to be between IX and X in MMI scale. More than eight cities and 1930 villages suffered damages as reported. The death toll surpassed 620 and thousands of people were injured. Sarpol-e Zahab city and its vicinities suffered most building damages and casualties.

Sarpol-e Zahab earthquake is just an example of natural catastrophic events that have occurred or can occur in urban area causing devastating damages in the future. Catastrophe modeling is a way to predict the consequences of any probable natural phenomena. It helps to improve short-term as well as long-term planning for disaster and risk management. These models need to be verified by actual events and observations. This paper presents a risk model for Sarpol-e Zahab earthquake to predict the building physical damages and the associated casualty loss. It also compares the results with some reconnaissance observations. For this purpose, OpenQuake platform is utilized for simulating the seismic scenarios. The fragility and vulnerability functions that were developed for the WP4 module (Risk Assessment Module) of GEM-EMME (Global Earthquake Model - Earthquake Model of the Middle East) project for Iran [5-6] were selected to predict physical damages. The global casualty model developed by Coburn et al. [7] has been modified according to local parameters and then applied to predict the human loss.

2. Reconnaissance

Damage Observation is a general term used in identifying and categorizing damages by human perception from a scene. This is also referred as Visual Damage Assessment. Ground Truth is referred to information provided by direct observation. However, in disastrous events where direct observation may take days and completed with exhaustive efforts, in other words time-consuming and expensive, damages can be deduced from visual study of Very High Resolution (VHR) satellite images more easily and relatively faster. This is done with the expense of omitting some obscured damages mostly because VHR optical satellites usually images the scene from the nadir position or with relatively smaller incidence angle.

UNITAR's Operational Satellite Applications Programme-UNOSAT team (mainly composed of GIS and imagery analysts, remote sensing experts, geologists, etc...) is delivering imagery analysis and satellite solutions for the purpose of humanitarian relief, human security, strategic territorial and development planning. For this event, UNITAR-UNOSAT has provided rapid damage maps of

hard hit cities and villages according to their protocol and resources [8]. Because of its nature that is related to the visual damage assessment from satellite imagery, the data always lacks the accuracy and the necessary detailing and needs to be cross checked/validated with the ground truth.

Google has developed and provided tools such as Google Person Finder, Google Crisis Map, Google Public Alerts, Google Maps, Google Earth, Google Fusion Tables, Google Docs, and Google Sites to help crisis responders and affected people to communicate and stay informed. For this event, Google Crisis Maps were published through Google services [9].

Sarpol-e Zahab Earthquake was felt by all western and central provinces in the country and also on tall buildings in Tehran. Eight cities, Ghasr-e Shirin, Ezgeleh, Salas-e Babajani, Gilan-e Gharb, Sarpol-e Zahab, Dalahoo, Eslamabad-e Gharb, Javanrood, and 1930 villages suffered destructive damages [3].

Sarpol-e Zahab city and two highly hit villages namely; Shahrak-e Zeraee and Ghara-Belagh-Azam, both adjacent to the northwest of the city were selected for this study. For this area, a reconnaissance trip has been conducted by the authors where the extent and the general aspects of building damages were observed. The construction types were mostly low-rise poor masonry or weak steel structures with infill brick walls.

In these areas, Shahrak-e Zeraee had experienced the most devastation with about an estimated figure of 60% damage ratio dominated by collapsed dwellings. This village experienced 35 deaths. For Ghara-Belagh-Azam, the destruction was slightly lower but accounted for at least 40%-50% and the death toll was 21.

In Sarpol-e Zahab city, the widespread destruction on poor quality buildings were reported and many recent constructions were collapsed. The northern-west area comprised of rather newly built dwellings but without proper earthquake resistance. The southern band of the city contained vulnerable older buildings mostly situated in older urban fabrics. In general, around 60% of buildings, mostly made of brick and weak steel frames in southern band and 20% to 30% on the northern band of Sarpol-e Zahab city were destroyed or seriously damaged and considered as total loss [10-11]. Figures (1) and (2) shows some of the collapsed buildings of the area.



Figure 1. Some of the collapsed buildings of Shahrak-e Zeraee.



Figure 2. Some of the collapsed buildings of Ghara-Belagh-Azam.

3. Seismic Loss Modeling

Science, technology, engineering knowledge, and statistical data are combined together to simulate the impacts of natural hazards in terms of damage and loss. Loss modeling is performed according to two general visions: 1) probabilistic, estimating the range of different potential catastrophes and their corresponding losses, and 2) deterministic, estimating the losses from single hypothetical or historical catastrophic event [12]. A scenario risk model generates a simulated event and estimates the amount of losses regarding magnitude, intensity, and location of the event concerning the elements at risk (inventory).

According to Equation (1), a loss model has three basic components namely hazard, exposure or inventory and vulnerability where their cross-influence indicates the expected loss. In following sections, each of the mentioned components are described for this case study.

$$\text{Seismic Loss} = \text{Seismic Hazard} \times \text{Exposure} \times \text{Vulnerability} \quad (1)$$

3.1. Seismic Hazard Assessment

In case of an earthquake scenario modeling, the

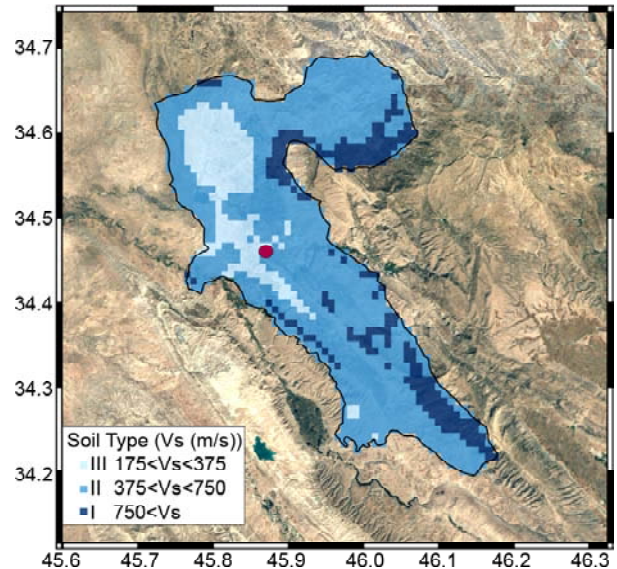


Figure 3. Soil classification of Sarpol-e Zahab sub-province based on USGS- V_{s30} adapted to Iranian Seismic Code 2800.

hazard component is estimated as the mean of the selected intensity parameter at sites of interest regarding the rupture and site parameters.

OpenQuake is employed to assess seismic hazard and risk in this study. In order to compute the hazard distribution, some soil parameters are required in GMPE equations. These parameters are the averaged shear wave velocity measured in the uppermost 30 meters of the soil column (V_{s30}) and depths to the 1 km/s and 2.5 km/s shear-wave velocity interfaces. In this research, the proxy method reflecting the correlation of V_{s30} to topographic slope "Global Slope-Based V_{s30} " as developed by USGS has been used [13-14]. Figure (3) displays the resulting soil classification based on Iranian seismic code 2800 in Sarpol-e Zahab sub-province.

Four ground motion prediction equations have been chosen for the region of study; Akkar et al. [15], Campbell and Bozorgnia [16], Chiou and Youngs [17] and Akkar and Cagnan [18]. The area under study

has been meshed with grids of 0.005° by 0.005° . The rupture is assumed to be a 25 by 60 km planar fault rupture according to the empirical relationship among magnitude with rupture surface [19]. The location of the rupture plane is set according to the IIEES report on rupture model of Sarpol-e Zahab earthquake [3]. To describe the attitude of the planar surface, the dip angle is assumed to be 14° , and the strike and rake angles are 351° and 137° according to USGS [2]. Figure (4) displays the map for the assumed rupture plane along with the known trace of MFF fault.

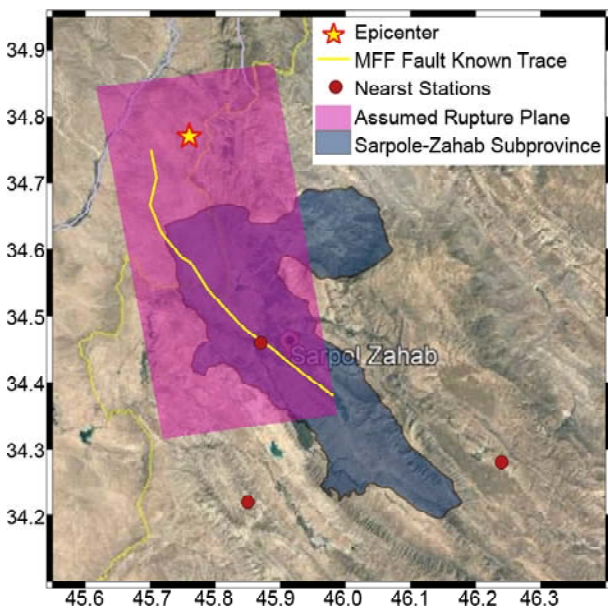


Figure 4. Plan view of assumed rupture plane and MFF fault known trace.

Figure (5) displays the resulting PGA map of Sarpol-e Zahab city and nearby villages from scenario hazard analysis. As it is seen, the PGA at SPZ station is estimated to be lower than the recorded PGA.

3.2. Population and Building Inventory

To prepare a GIS-based building inventory for loss modeling, "population" and "building" data sets are required. Information on the physical characteristics of the elements at risk typically consists of structural type, construction year, number of stories, occupancy, number of occupants, etc.

In Iran, a quinquennial national census program updates the national population and building statistics with some limited spatial and attribute details. The latest published census data (2016) was collected from survey forms and relevant to housing units. In this dataset, building statistics are presented for administrative divisions of provinces and sub-provinces.

Although the national census program data collection covers the whole country in both rural and urban areas and usually with a high rate of citizen's contribution, there are always some shortcomings. The current census data collection in the country lacks the accuracy and the completeness for it is based on filling quick survey questionnaires. Not all surveyors have the required expertizes to assess the buildings attributes correctly, and in many cases the owners

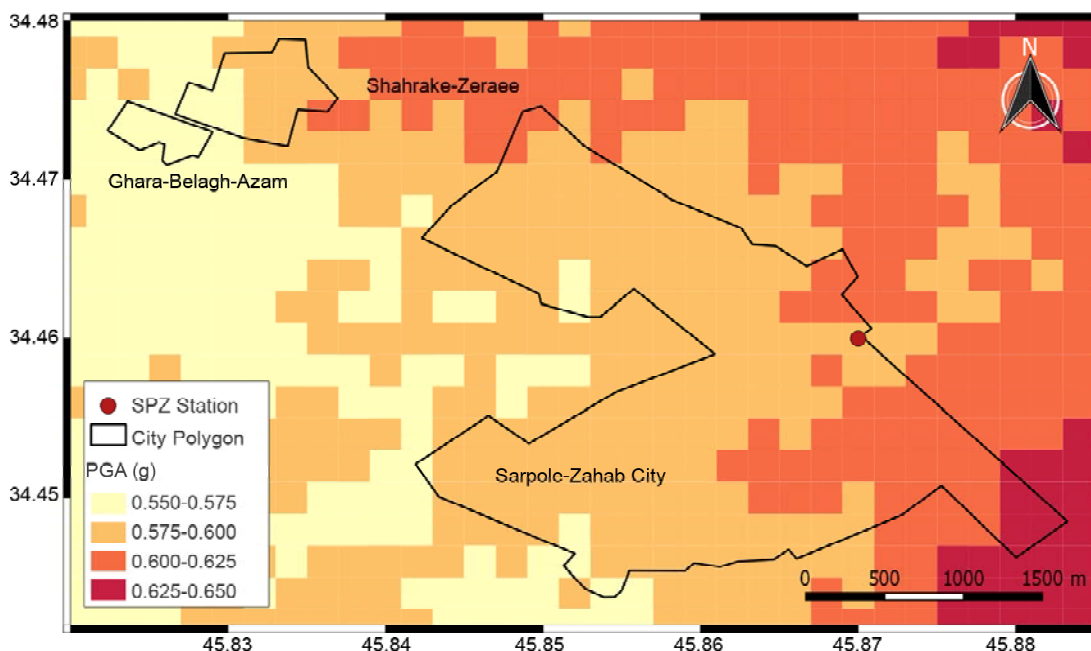


Figure 5. Simulated PGA distribution of Sarpol-e Zahab city with neighboring villages.

have very limited knowledge in answering to the questions properly. Besides, considering the covering and the claddings in the typical structures, the building type assignment has a tendency to be from guesses. Moreover, the questionnaires do not reflect all required information to create an ideal building inventory. Furthermore, such forms are based on housing unit statistics and do not reveal information regarding individual buildings (i.e. no data indicating the number of stories for the building stock).

Nevertheless, the national census program provides very useful information and statistics for large scale risk analysis. The compilation of housing statistics along with the population distribution data sets such as LandScan database (worldwide grid population) [20] create a geospatial database with uniform spatial resolution through a process of dasymetric mapping. In this technique, a coarser spatial data is disaggregated to a finer spatial units conserving relative homogeneity. In this paper, LandScan 2014 global population database at 30 arc-seconds (1 km or finer) is used for Sarpol-e Zahab sub-province. This grid data is calibrated according to the national census data according to a procedure suggested by Mansouri and Amini-Hosseini [21]. The building inventory is created in grid format concerning the regional distribution statistics and the norms and patterns for the residential population.

Based on 2016 census data, the population of Sarpol-e Zahab sub-province and Sarpol-e Zahab city is 85342 and 45481, respectively. Figure (6) represents the gridded population of Sarpol-e Zahab sub-province from LandScan 2014 as calibrated by the 2016 national population census data.

The building typology of National census database is provided as: "Steel structures", "Concrete structures", "Etc." and "Unknown". "Etc." type includes 'brick and steel or stone and steel', 'brick and wood or stone and wood', 'cement block', 'brick with or without stone', 'wooden', 'adobe and wood', 'adobe' and 'etc.'.

GEM-EMME fragility and vulnerability curves for Iran [5-6] are selected to estimate the consequences of simulated scenario. In this classification for Iranian building typology, buildings are categorized in four general classes of Adobe, Masonry, Steel Frame and Concrete Frame. Some of these classes are graded based on levels of

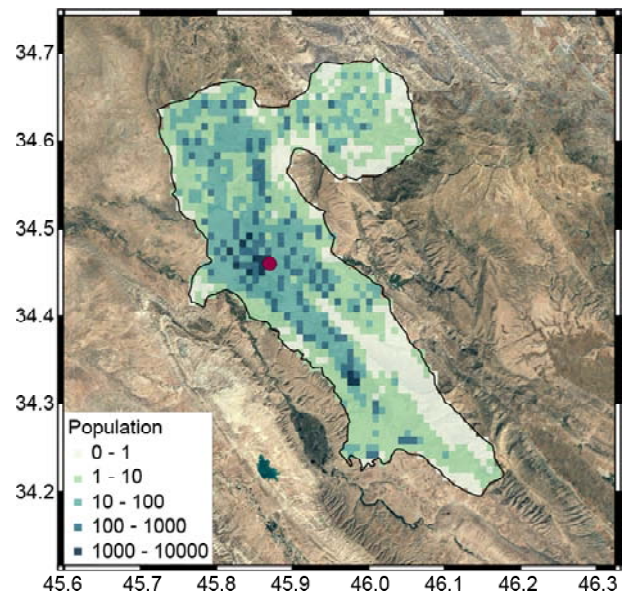


Figure 6. Calibrated LandScan 2014 gridded population of Sarpol-e Zahab sub-province.

earthquake resistant design or quality of construction as poor, mediocre and good quality of construction. It is assumed that the construction quality of steel and concrete frame buildings is poor, mediocre and good if they have been built before 1996, between 1996 and 2006 and after 2006, respectively. The selected building typology tags for these building subclasses are S3, S2 and S1 for steel frames and C3, C2 and C1 for concrete frames. Masonry buildings are divided into two classes of unreinforced masonry (M23) and reinforced masonry (M1), which have poor and good construction quality respectively. Adobe buildings (AD) built at all times are assumed to be extremely vulnerable. Based on the norm for the building construction in the area, it is assumed that buildings of different types are low- or mid-rise.

According to the field surveys and refining/ comparing the databases for the last two national census programs, it is inferred that "brick and steel or stone and steel" buildings have mostly weak steel structures. Consequently, they have been categorized as poor steel construction (S3). It is also assumed that "Unknown" building typologies have a similar seismic behavior to M23 (poor masonry) buildings. Table (1) shows the structural typology tags as assigned to the census building classification.

Figure (7) depicts the buildings parcel map of Sarpol-e Zahab city and nearby villages provided basically by OpenStreetMap, where some modi-

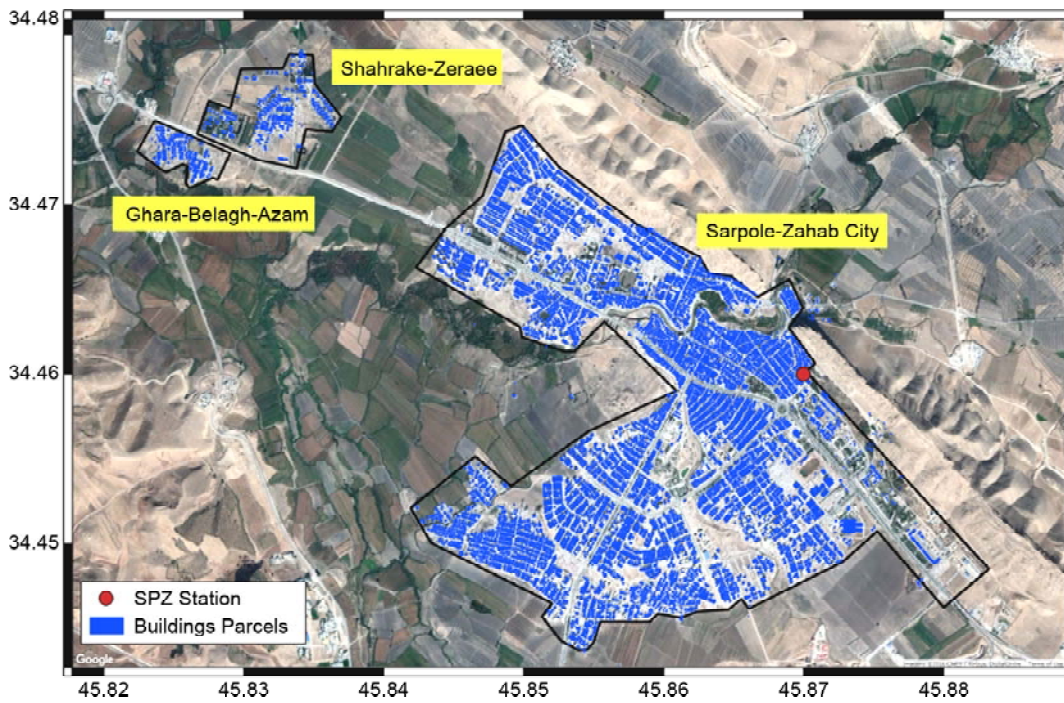


Figure 7. Buildings parcel map of study region - according to OpenStreetMap with some modifications.

Table 1. Building typology tag assignment.

Census Typology Tag	Structural Tag
Steel Structure	S
Concrete Structure	C
Brick and Steel or Stone and Steel	S3
Brick and Wood or Stone and Wood	M23
Cement Block	M23
Brick with or without Stone	M23
Etc.	M23
Wooden	M23
Adobe and Wood	AD
Adobe	AD
Etc.	AD
Unknown	M23

fications and additions were made in this study. From this map, the total number of buildings in Sarpol-e Zahab city is counted as 9635. Studying the 2016 census data, 12850 housing units are reported for this city. It should be noted that there are always sources of errors in the census database, some building footprints are associated with multi-story constructions and/or some of the buildings have different land-use other than residential. Considering a portion of parcels as non-residential buildings, it is estimated that the number of housing units is less than 2 times of buildings in overall sense. This rough estimation indicates that the building stock is dominated by low-rise buildings.

Nevertheless, some few mid-rise buildings were observed that are mostly among new constructions. For Shahrak-e Zeraee, 167 households were recorded in the census data while the count of building parcels was 277 from the modified OpenStreetMap. The 2016 national census indicated 203 households in Ghara-Belagh-Azam that matched well with the number of building footprints as observed from satellite images.

Classifying the housing data according to the construction year will reflect also the quality of the construction because of aging and also the level of earthquake design/practice being implemented in different epochs. Unfortunately, for the most recent census program (2016), the construction year has not been collected nor reported. As an alternative, the building census data of 2011 has been utilized as a complementary dataset for it reflects the construction year for major portions of the building taxonomy. Table (2) shows the number of housing units regarding typology and construction year based on census 2011 data, and Table (3) represents the difference in total number of different building types between the two consecutive census programs. As it is seen, due to the significant differences in the total numbers, one cannot simply infer that positive differences would be equivalent to new constructions during this 5-year period, or negative differences

Table 2. Number of housing units according to typology and construction year for 2011 Census.

Construction Year	Total	Steel	Concrete	Etc.									
				Brick and Steel or Stone and Steel	Brick and Wood or Stone and Wood	Cement Block	Brick with or without Stone	Wooden	Adobe and Wood	Adobe	Etc.	Unknowm	Unknown
sum	19442	1658	633	16945	13029	2340	349	519	2	282	266	19	139
2011	304	68	28	208	178	14	9	1				2	4
2010	670	154	36	478	404	28	25	14				1	6
2009	853	119	116	617	500	58	21	23		4	4		7
2008	824	65	54	703	593	59	20	17		4	4	1	5
2007	982	71	110	799	674	62	19	21		4	7		12
2006	1962	179	137	1644	1253	240	55	26		31	24	2	13
1996-2005	6786	514	107	6162	4814	791	142	165		78	124	9	39
1986-1995	5247	387	35	4820	3669	741	47	165	1	106	55	2	34
1976-1985	996	83	4	907	505	243	6	69	1	41	31	2	9
1966-1975	425	7		417	324	63	3	5		9	12		1
Before 1966	50	3		47	10	25	1			4	3		4
Unknown	343	8	6	143	105	16	1	13		1	2		5

Table 3. Difference in building types between two consecutive census programs.

Census Year	Total	Steel	Concrete	Etc.									
				Brick And Steel or Stone and Steel	Brick And Wood or Stone and Wood	Cement Block	Brick With or Without Stone	Wooden	Adobe and Wood	Adobe	Etc.	Unknowm	Unknown
2011	19442	1658	633	13029	2340	349	519	2	282	266	19	139	206
2016	21996	5663	4117	8762	1162	721	766	16	376	193	195		25
Difference	2554	4005	3484	-4267	-1178	372	247	14	94	-73	176	-139	-181

cannot be justified as destruction. The main reason is believed to be mostly due to census data collection level of expertise. As an example, the total number of "Unknown" structures has been reduced in census program 2016. In order to make use of the distribution of buildings age from the census 2011 data, some steps were taken. First, in cases where such differences were positive, the number of building units constructed during recent five years was assumed to be the same as the past five years considering the construction increase rate, of about 13 percent. The residual has been distributed for all construction periods regarding the relative abundance of each data bin (temporal data). Negative differences were observed in building types assumed to have low quality regardless of their construction year. They have been simply subtracted from the total amount of census data 2011. Table (4) represents the final distribution of different building types for this study.

A known source of possible errors is due to inevitable assumptions that must be made in order to complete and to classify the building typology and the associated structural attributes into distinguishable taxonomies. Such assumptions will certainly affect the results of risk/loss computation. Nonetheless, it is worth evaluating the significance of such misclassification into the final results. For example, assigning the "brick and steel or stone and steel" as M23 rather than S3, would have around 13 percent higher estimated loss for that specific class and about 5 percent when considering the entire portfolio. Taking "Unknown" building class as M23 seems logical because usually unknown structural types refer to the older building stocks (frameless structures) where the owners or the surveyor are not able to distinguish or identify. In this case, if the "unknown" buildings are tagged as other structural class, the deviation in the final results would have been insignificant, for that less than 0.1 percent of

Table 4. Final distribution of different building types (housing units) for this study.

Building Typology	Total Number of Housing Units	Percent
AD	764	3.5
M23	2690	12.2
S1	4405	20.0
S2	1211	5.5
S3	8808	40.0
C1	3936	17.9
C2	157	0.7
C3	24	0.1
Sum	21996	100

the entire stock is actually reported as "Unknown". Moreover, it has been assumed that there is no reinforced masonry building (M1) in the study area; therefore, the age of the construction would affect only the steel and concrete classes that represent almost 84 percent of the building stock. The result of an extreme case of misclassifying a sample "poor quality" steel or concrete frame (S3 or C3) as "good quality" (S1 or C1), would cause 62 percent and 54 percent estimated lower loss, respectively for that individual building. It should be pointed out that the building pool is always a blend of buildings with various ages and different engineering practices that tend to average out the results.

3.3. Physical Loss Assessment

A vulnerability curve is a relation between the building damage or loss and an earthquake intensity parameter such as PGA. For the vulnerability assessment, it is necessary to categorize the building types and to assign the vulnerability functions accordingly. As described earlier, major building types in Iran are adobe, masonry, reinforced concrete and steel. For GEM-EMME building typology tailored for Iran, damage curves were derived using the EMS-98 procedure and calibrated for empirical and analytical results and expert judgment [5-6]. Figure (8) represents the expected damage ratio of

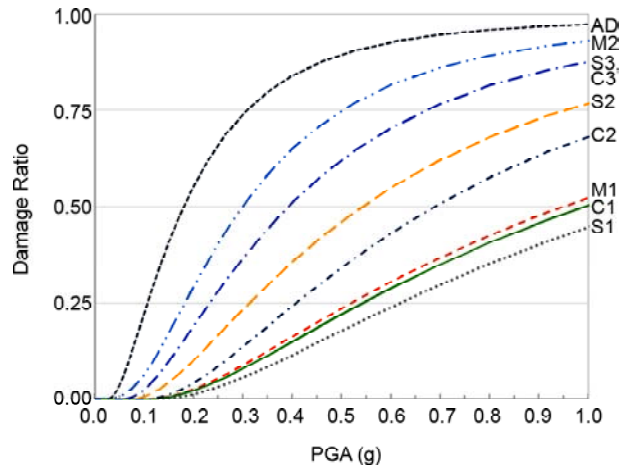


Figure 8. Expected damage ratio of different building types [5-6].

different building types.

In this research, the expected physical loss ratio of buildings of Sarpol-e Zahab and nearby villages has been assessed with two hazard inputs: 1) the estimated PGA distribution from earthquake scenario modeling, and 2) uniform PGA distribution equal to the recorded PGA at SPZ station.

For developing spatially distributed building inventory, two distinct methods were employed in this study. The first scheme used the aforementioned calibrated LandScan grid map. This scheme is suited for larger scale calculations (i.e. regional or country wide database setup) that would otherwise be hardware demanding and time consuming. Figure (9) depicts the expected physical loss ratio map corresponding to the LandScan grids as calibrated to the census statistics for 2016. Besides, a method envisaging the building footprints as building parcels (Figure 7) has been employed for its comparable better and finer resolution of the building stock. The parcel-scale distribution of the expected physical loss ratio is depicted in Figure (10).

The total physical loss ratio has been estimated to be 45 percent for the case where spatially distributed PGA is modeled. Table (5) represents the

Table 5. Damage state distribution of buildings.

Damage State	Damage Ratio Range	Building Typology							
		AD	M23	C1	C2	C3	S1	S2	S3
D5	100	73.3	45.6	1.5	5.0	26.2	2.8	11.0	26.2
D4	60-100	21.2	36.8	14.1	25.5	40.9	19.6	34.7	40.9
D3	20-60	4.8	14.1	31.5	35.8	24.0	34.6	33.5	24.0
D2	1-20	0.7	3.2	33.6	25.0	7.7	29.8	16.8	7.7
D1	0-1	0.0	0.3	17.3	8.1	1.1	12.1	3.8	1.1

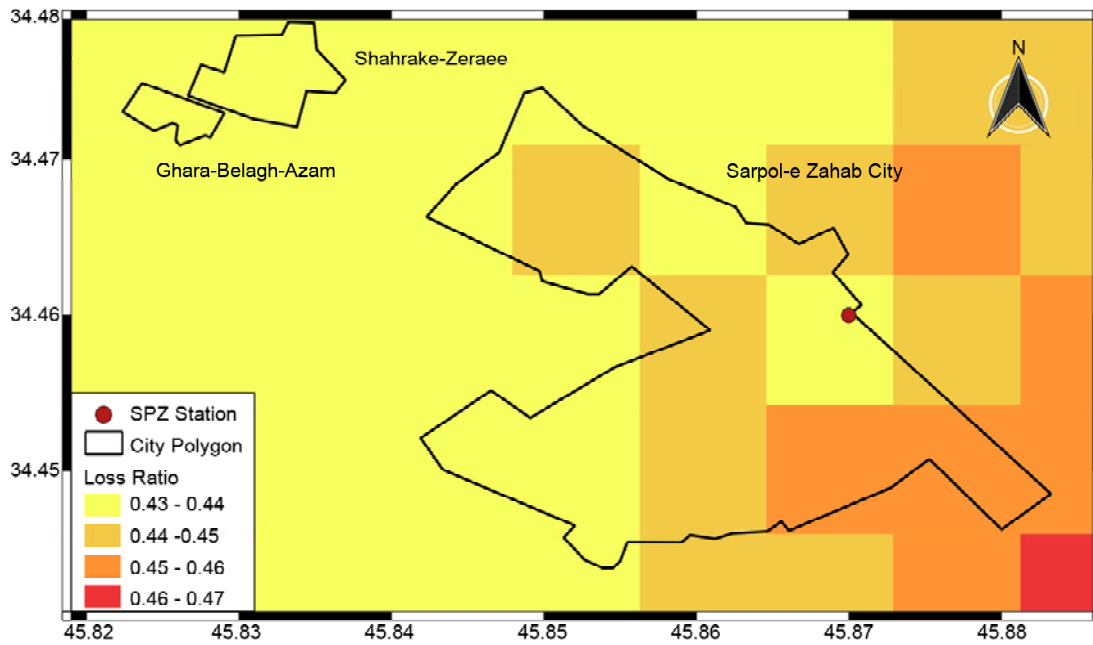


Figure 9. Grid-based distribution of expected physical loss ratio.

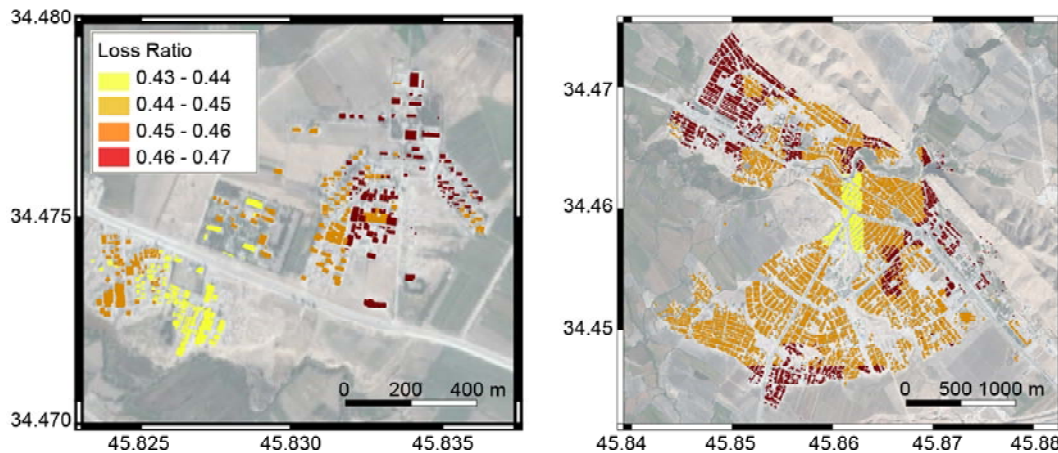


Figure 10. Parcel-based distribution of expected physical loss ratio of Sarpol-e Zahab city (right) and nearby villages (left).

approximate percent of buildings in each damage state. When the uniform and constant PGA of 0.697 g is accounted for the hazard input, the estimated physical loss ratio resulted in 60 percent.

3.4. Human Loss Assessment

According to Coburn and Spence human loss model [7], the "lethality ratio" of building stock must be determined to estimate the casualties due to earthquakes. This is the ratio of the number of people killed to the number of occupants present in collapsed buildings at the time of the earthquake. Equation (2) calculates the human loss for each building type. In order to estimate the proportions of the people rescued and trapped at each stage, a set of M-parameters is used. D5 is the total number of

collapsed structures. Figure (11) shows D5 as a function of PGA for different building types according to a study completed by Mansouri and Amini-Hosseini [21], and Mansouri et al. [6]. Table (6) shows the M-parameters determined for Sarpol-e Zahab earthquake human loss modeling. The ratios of occupancy at time of earthquake (M2) and proportion of occupants trapped by collapse (M3) are determined regarding to the preparedness of people due to the several foreshocks.

$$Ks = D5 \times [M1 \times M2 \times M3 \times (M4 + M5(1 - M4))] \quad (2)$$

The result for human loss estimation along with observed casualties is summarized in Table (7).

Table 6. Determined M-parameters for human loss estimation.

Parameter	Description	Engineering Buildings	Non-Engineering Buildings
M1	Population Per Building		-
M2	Occupancy at Time Of Earthquake		0.7
M3	Proportion of Occupants Trapped by Collapse		0.2
M4	Proportion of Occupants Killed at Collapse	0.4	0.2
M5	Mortality Post-Collapse	0.8	0.55

Table 7. Recorded and estimated casualties.

Location	Population (National Census)	Reported Casualty (Killed)	Estimated Casualty	
			Model Distributed PGA	Uniform PGA (Recorded)
Sarpole-Zahab	45481	<500	1046	1423
Ghara-Belagh-Azam	803	21	18	25
Shahrake-Zeraee	681	35	15	21
sum	46965	<550	1079	1470

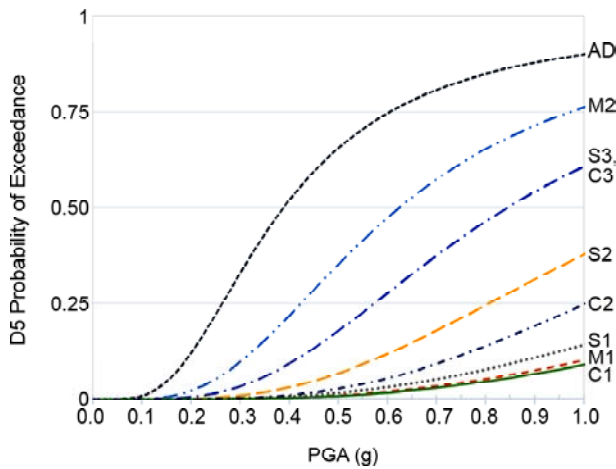


Figure 11. Variation of D5 with PGA for different building types [5-6].

To calculate the estimated human loss, both approaches of PGA distribution (as described in section 3.3) have been considered.

The total estimated human loss in both methods are higher than the reported actual death toll. One major justification can be the lack of data related to missing persons. The death toll mostly covers only the recorded death by medical jurisprudence authority or other medical organizations, and potentially does not reflect accurately the number of burials by the local people considering critical post-event situations. Therefore, the reported casualty data is usually underestimated. On the other hand, the population for the study area at the time of the event is not necessarily equivalent to the census data. Another noteworthy factor is the very high sensitivity of the casualty result to the uncertain input parameters as D5 and all M-parameters. The

building damage and the casualty modeling have sources of aleatory and epistemic uncertainties. Moreover, the consequences of destructive earthquakes cannot be completely and accurately modeled utilizing only a few parameters. For example, a peak ground acceleration value is used as the only parameter to describe the ground shaking severity.

4. Conclusion

Catastrophe loss modeling is an important component of any risk management strategy. It is the process of calculating the estimated loss due to a catastrophic event such as an earthquake. Loss modeling helps the authorities to predict, manage and mitigate damages due to natural events. The best approach to verify a loss model is to compare and to calibrate the estimated results with actual/empirical outcomes. This paper presents an earthquake model to predict the building physical damages and the associated casualties for the case of Sarpol-e Zahab. A high PGA value of 684 gal has been recorded for at the SPZ station (in Sarpol-e Zahab city), and also some adequate field surveys and documentations were completed for this event. OpenQuake platform has been employed to calculate a distribution of ground motion intensity considering the sources and some inferred site conditions. A spatial building database has been developed by dasymmetric mapping technique by merging a grid world population distribution map and the national census data. OpenQuake platform has been also utilized to

simulate the ground motion field and to assess the physical damages and human loss. The total physical loss ratio between 45 to 60 percent were estimated for residential buildings. Poor quality of construction of buildings is the main source of devastations. It is evaluated that 95 percent of adobe buildings and 82 percent of unreinforced masonry buildings experienced unrepairable damages. The results have been compared with the actual observed data showing a relative proper match. The ratio of people killed to the number of people present at the region of study at the time of earthquake is estimated as 0.023. The total expected human loss as calculated by the global model overestimates the actual figure. This is believed because people have been alert by some foreshocks and many quitted their home thereafter, and also because some levels of training were introduced (i.e. school earthquake drills) to the citizens.

Some additional future researches will be beneficial in enhancing the outcomes of this present investigation. A more complete soil information (or model) and site effect evaluation will help in calculating the ground shaking intensity distribution more accurately. Moreover, the development of a building database reflecting individual building information in detail is desired. Considering the local construction practice, it will be useful to develop fragility curves and vulnerability functions for the nominal building taxonomies specific to the study area. The vulnerability functions utilized in this present work have been derived previously according to the typical building inventory for the country. Recently, some relevant studies have started to model the seismic performance of the local existing buildings and also to derive the empirical fragility functions associated to the 2017 Sarpol-e Zahab earthquake. This current work may be regarded as the risk/loss computation engine to assist a future disaster monitoring in a systematic manner.

Acknowledgment

This research is completed under the International Institute of Earthquake Engineering and Seismology sponsorship to study the Nov. 12, 2017 Sarpol-e Zahab earthquake. It also represents a partial risk assessment verification of the IIEES project activated under the research contract number

687-8122.

LandScan is the community standard for global population distribution and the data has been used for the area of interest in this research. The LandScan Global Population Database has been developed by the Department of Energy's Oak Ridge National Laboratory Oak Ridge National Laboratory, Oak Ridge, TN, < <http://www.ornl.gov/sci/landscan/> >.

OpenQuake platform has been employed for seismic hazard and risk computation in this study. This platform and the computation engines were developed under the Global Earthquake Model (GEM) foundation as a free open source package.

OpenStreetMap is an open license map of the world created by people under the Open Data Commons Open Database License (ODbL) by the OpenStreetMap Foundation (OSMF).

References

1. Iranian Seismological Center (IRSC) (2017) *Magnitude 7.3, Kermanshah Province 2017*. Available from: http://irsc.ut.ac.ir/newsview.php?&eventid=125729&network=earth_ismc__.
2. USGS (2018) *M 7.3 - 29 km S of Halabjah, Iraq 2017*. Available from: <https://earthquake.usgs.gov/earthquakes/eventpage/us2000bmcg#moment-tensor>.
3. Tatar, M., Ghaemaghmanian, M., Yamini-Fard, F., Hesami-Azar, K., Ansari, A., and Firoozi, E. (2018) *2017 Sarpol-e Zahab Earthquake Report - Seismology Aspects*. IIEES.
4. Road Housing & Urban Development Research Center (2017) *Sarpol-e Zahab*. Available from: <http://smd.bhrc.ac.ir/Portal/fa/BigQuakes/Details/125>.
5. GEM (2013) *Earthquake Model of the Middle East Region (EMME) WP4: Seismic Risk Assessment*.
6. Mansouri, B., Kiani, A., and Amini-Hosseini, K. (2014) A Platform for earthquake risk assessment in Iran case studies: Tehran scenarios and Ahar-Varzeghan earthquake. *Journal of Seismology and Earthquake Engineering*, **16**(1), 51-69.
7. Coburn, A.W., Spence, R.J., and Pomonis, A. (1992) Factors determining human casualty

- levels in earthquakes: mortality prediction in building collapse. *Proceedings of the First International Forum on Earthquake Related Casualties*, Madrid, Spain.
8. United Nations Institute for Training and Research. Available from: www.UNITAR.org.
 9. Google Crisis Map, *Iran-Iraq Earthquake*.
 10. Seymoradi, H. (2018) Debris Monitoring Field Supervisor of Housing Foundation of Islamic Revolution, *Personal Communication*.
 11. Hoseini Hashemi, B., Mansouri, B., Kalantari, A., and Sarvghad-Moghadam, A. (2018) *2017 Sarpol-e Zahab Earthquake Report-Structures and Life Lines*. IIEES.
 12. Risk Management Solutions (RMS) (2015) *What is Catastrophe Modeling?* [cited 2018; Available from: <http://www.rms.com/blog/2015/06/22/what-is-catastrophe-modeling/>].
 13. Allen, T.I. and Wald, D.J. (2009) On the use of high-resolution topographic data as a proxy for seismic site conditions (V_{s30}). *Bulletin of the Seismological Society of America*, **99**(2A), 935-943.
 14. Worden, C.B., Wald, D.J., Sanborn, J., and Thompson, E.M. (2015) Development of an open-source hybrid global V_{s30} model. *Seismological Society of America Annual Meeting*. Pasadena, California.
 15. Akkar, S., Sandikkaya, M., and Bommer, J. (2014) Empirical ground-motion models for point-and extended-source crustal earthquake scenarios in Europe and the Middle East. *Bulletin of Earthquake Engineering*, **12**(1), 359-387.
 16. Campbell, K.W. and Bozorgnia, Y. (2008) NGA ground motion model for the geometric mean horizontal component of PGA, PGV, PGD and 5% damped linear elastic response spectra for periods ranging from 0.01 to 10 s. *Earthquake Spectra*, **24**(1), 139-171.
 17. Chiou, B.S.-J. and Youngs, R.R. (2014) Update of the Chiou and Youngs NGA model for the average horizontal component of peak ground motion and response spectra. *Earthquake Spectra*, **30**(3), 1117-1153.
 18. Akkar, S. and Cagnan, Z. (2010) A local ground-motion predictive model for Turkey, and its comparison with other regional and global ground-motion models. *Bulletin of the Seismological Society of America*, **100**(6), 2978-2995.
 19. Wells, D.L. and Coppersmith, K.J. (1994) New empirical relationships among magnitude, rupture length, rupture width, rupture area, and surface displacement. *Bulletin of the Seismological Society of America*, **84**(4), 974-1002.
 20. Oak Ridge National Laboratory, <http://web.ornl.gov/sci/landscan>.
 21. Mansouri, B. and Amini-Hosseini, K. (2012) Development of residential building stock and population databases and modeling the residential occupancy rate for Iran. *Natural Hazards Review*, **15**(1), 88-94.